

This document is confidential and is proprietary to the American Chemical Society and its authors. Do not copy or disclose without written permission. If you have received this item in error, notify the sender and delete all copies.

Identification of Novel 'Inks' for 3D Printing Using High Throughput Screening: Bioresorbable Photocurable Polymers for Controlled Drug Delivery

Journal:	<i>ACS Applied Materials & Interfaces</i>
Manuscript ID	am-2017-15677w.R1
Manuscript Type:	Article
Date Submitted by the Author:	19-Dec-2017
Complete List of Authors:	<p>Louzao, Iria; Universidade de Santiago de Compostela, Organic Chemistry Koch, Britta; The University of Nottingham, Laboratory of Biophysics and Surface Analysis Taresco, Vincenzo; University of Nottingham, Pharmacy Ruiz Cantu, Laura; the university of nottingham, pharmacy Irvine, Derek; University of Nottingham, School of Chemistry and School of Chemical and Environmental Engineering Roberts, Clive; The University of Nottingham, School of Pharmacy Tuck, Christopher; University of Nottingham, Department of Mechanical, Materials and Manufacturing Engineering Alexander, Cameron; University of Nottingham, School of Pharmacy Hague, Richard; The University of Nottingham, UK, Mechanical, Materials and Manufacturing Engineering Wildman, Ricky; University of Nottingham, Department of Chemical and Environmental Engineering Alexander, Morgan; The University of Nottingham, Laboratory of Biophysics and Surface Analysis</p>

SCHOLARONE™
Manuscripts

1
2
3
4
5
6
7 Identification of Novel ‘Inks’ for 3D Printing Using
8
9
10
11 High Throughput Screening: Bioresorbable
12
13
14
15 Photocurable Polymers for Controlled Drug
16
17
18
19 Delivery
20
21
22
23

24 *Iria Louzao, ‡§† Britta Koch, ‡ Vincenzo Taresco, ‡ Laura Ruiz-Cantu, § Derek J. Irvine, § Clive J.*
25
26 *Roberts, Christopher Tuck, § Cameron Alexander, ‡ Richard Hague, § Ricky Wildman § and*
27
28 *Morgan R. Alexander ‡**
29
30
31

32 AUTHOR ADDRESS ‡School of Pharmacy and §Faculty of Engineering, University of
33
34 Nottingham, Nottingham NG7 2RD (UK).
35
36
37

38 KEYWORDS: 3D printing, Drug Delivery, Polymer materials, Biomedical devices, Sustained
39
40 drug release.
41
42
43

44 ABSTRACT A robust discovery methodology is presented to identify novel biomaterials
45
46 suitable for 3D printing. Currently the application of Additive Manufacturing is limited by the
47
48 availability of functional inks, especially in the area of biomaterials-this method tackles this
49
50 problem for the first time allowing hundreds of formulations to be readily assessed. Several
51
52 functional properties, including the release of an antidepressive drug (paroxetine), cytotoxicity
53
54 and printability are screened for 253 new ink formulations in a high-throughput format as well as
55
56
57
58
59
60

1
2
3 mechanical properties. The selected candidates with the desirable properties are successfully
4 scaled up using 3D printing into a range of object architectures. A full drug release study,
5 degradability and tensile modulus experiments are presented on a simple architecture to
6 validating the suitability of this methodology to identify printable inks for 3D printing devices
7 with bespoke properties.
8
9
10
11
12
13
14
15
16
17
18

19 **Introduction**

20
21 Additive Manufacturing, often termed 3D printing, is emerging as a technology with great
22 potential for the manufacture of bespoke medical devices. Whilst there is some progress in
23 identifying new materials for 3D printing,¹⁻⁴ progress is slow and a limitation remains in the lack
24 of functional materials that can currently be printed.⁵⁻¹⁰ To address this challenge, we propose a
25 high throughput screening approach to identify “inks” for 3D printing of functional materials.
26 We exemplify this by targeting the identification of polymers printable using UV photo initiation
27 for optimal bioresorbable drug delivery devices. The approach involves high throughput
28 screening of a library of materials deposited as small polymer spots arranged as micro arrays,
29 which are then used to identify which of the materials have the appropriate mechanical and cell
30 compatibility properties. This surface-focused micro array screening approach is complemented
31 by assessing larger samples in well-plates for bulk performance determination, which in this
32 exemplification of the approach was quantification of drug release. From these high-throughput
33 screening of different properties, 19 materials were shortlisted. A final selection was made based
34 on an estimate of the printability, which led to the identification of materials that could be scaled
35 up for 3D printing. Hit materials from the library were then used to fabricate drug-containing
36
37
38
39
40
41
42
43
44
45
46
47
48
49
50
51
52
53
54
55
56
57
58
59
60

1
2
3 objects suitable for subcutaneous implantation.¹¹ Release profiles from these objects were
4
5 quantified by standard drug dissolution testing procedures, illustrating the success of this
6
7 approach in identifying new inks ready for use in the manufacture of bioresorbable medical
8
9 devices by 3D printing.¹² To the best of our knowledge, this is the first high throughput screening
10
11 approach described for identifying inks for 3D printing or bioresorbable drug delivery polymers.
12
13 The method illustrated here offers opportunities in many other fields where new functional 3D
14
15 printable materials are required.
16
17
18
19
20

21 The main advantage of additive manufacturing with respect to traditional manufacturing
22
23 techniques is the freedom of object design, providing an ideal opportunity for manufacturing
24
25 personalized medicines¹³ and devices.^{14,15} Of the 3D printing technologies available, jetting of
26
27 liquid *inks* to form solid materials¹⁶ enabled by piezoelectric inkjet methods allows for superior
28
29 resolution^{17,18} when compared to other popular techniques such as extrusion (often used for
30
31 bioprinting/cell printing).¹⁹⁻²¹ However, the range and functionality of materials available for
32
33 inkjet printing are limited and a major barrier to the adoption of new materials is the printability
34
35 requirements of a particular ink formulation, which needs to meet physical and rheological
36
37 constraints in order to be ejectable from a nozzle.^{22,23}
38
39
40
41
42
43

44 Herein we explore a library of copolymers based on acrylated oligo or poly (β -amino ester)²⁴⁻²⁶
45
46 photo curable macromers (abbreviated to PBAE) and acrylic monomers, to identify suitable
47
48 photocurable 3D printable ink formulations with a range of drug release properties. These
49
50 bioresorbable materials based on acrylated β -amino esters (Figure 1a) are oligomeric (macromer)
51
52 products from a Michael addition reaction and have enormous potential in applications where the
53
54
55
56
57
58
59
60

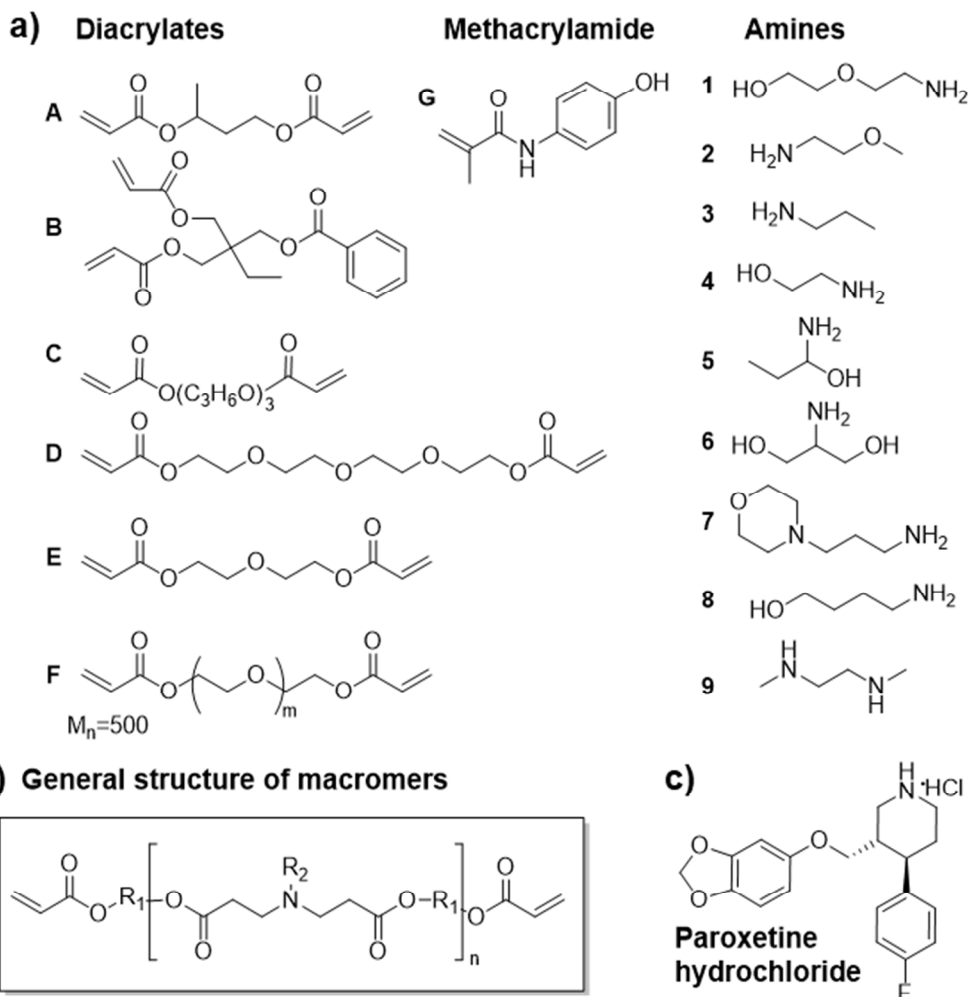
1
2
3 polymer is required to hydrolytically degrade in service, such as during or after drug delivery
4
5 from an implant. To illustrate this, we have chosen paroxetine hydrochloride (Figure 1c), an
6
7 antidepressant drug in a group of medicines called selective serotonin reuptake inhibitors. To
8
9 overcome side effects related to treatments with paroxetine, such as cardiac arrhythmia or
10
11 insomnia, extended release from a subcutaneous implant is a desirable strategy to reduce these
12
13 serious side effects possible from oral systemic delivery over long periods of time.^{27,28} For our
14
15 illustration of a high throughput screening study this drug has the advantage that it is auto
16
17 fluorescent allowing us to use fluorescence spectrophotometry to quantify the drug released, but
18
19 the 384 well plate format allows for the analysis of any compound using auto sampling methods
20
21 and quantification by high performance liquid chromatography mass spectrometry. By
22
23 examining drug release from well plated for up to 2 months in vitro, in addition to high
24
25 throughput analysis of cytotoxicity and modulus, we selected candidate materials for scale-up to
26
27 3D printing which were further refined by consideration of the printability of the inks. Objects
28
29 suitable for subcutaneous implantation were successfully printed into a variety of forms with the
30
31 selected ink and subjected to macroscopic tensile mechanical testing, drug release and polymer
32
33 degradation studies.
34
35
36
37
38
39
40
41

42 **Results and Discussion**

43 **Polymer library synthesis and micro array fabrication**

44
45
46
47 PBAEs are easily synthesized in bulk by a Michael addition reaction of primary amines (or a
48
49 bis(secondary) amine) with diacrylates following the approach of Anderson *et al.*²⁴ (Figure 1ab).
50
51
52
53
54 The diacrylates were used in excess in order to preserve acrylate functionalities at both ends. A
55
56
57
58
59
60

total of 6 diacrylates (A-F, Figure 1a) and 6 amines (1-6, Figure 1a) were combined at 1.2 :1 diacrylate/amine molar ratio to give rise to 36 macromers in principle, identified as diacrylate-amine (letter-number) code according to Figure 1a (Table S1, Supporting Information). To further explore the effect of composition, the diacrylate/amine ratio was also modified to 1.2:1, 1.5:1 and 2:1 in one case (identified as C3, C3-15 and C3-2 respectively). Diacrylate C was further combined with another three amines 7-9 to form a total of 42 macromers.



1
2
3 **Figure 1.** (a) Chemical structures of the diacrylates (*A-F*) and amines (1-9) used to synthesise
4 the PBAE macromers and methacrylamide *G*. (b) General structure of PBAE macromers. (c)
5
6
7
8
9
10
11
12
13
14
15
16
17
18
19
20
21
22
23
24
25
26
27
28
29
30
31
32
33
34
35
36
37
38
39
40
41
42
43
44
45
46
47
48
49
50
51
52
53
54
55
56
57
58
59
60

Chemical structure of paroxetine hydrochloride.

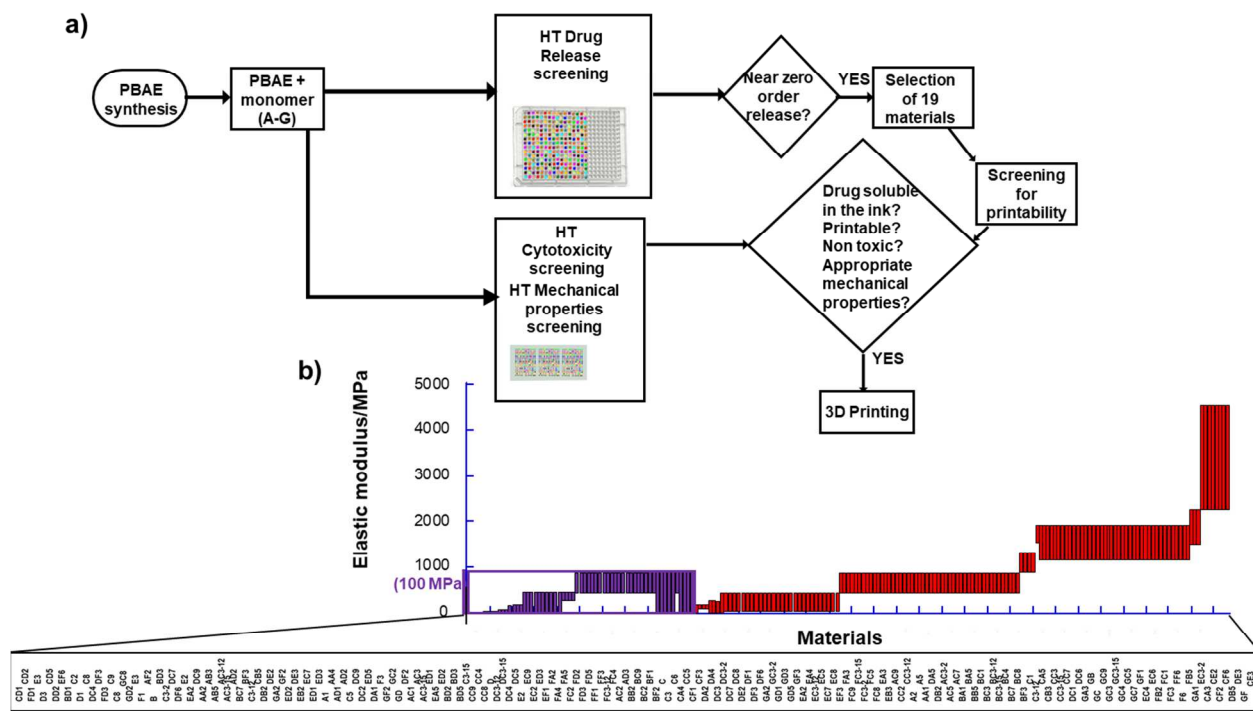
While piezoelectric 3D printing is highly sensitive to ink viscosity, this is not the case with pin-printing where grooved reservoirs in metal pins are filled by capillary forces on immersion into liquid inks. This technique allows for microarray preparation of a very wide range of inks which we printed prior to high throughput characterization of the UV cured spots in the accessible form of a polymer micro array.²⁹⁻³⁴ Pure PBAE are in general too viscous for piezoelectric ink jet printing. The microarray strategy allows for the rapid screening of a large amount of materials by combining PBAE and diacrylate monomers (*A-F*).

Combinatorial mixtures of 42 PBAEs and 6 diacrylates and one acrylamide (mixed with both PBAE and diacrylates, Figure 1a) gave rise to 253 materials. To prepare the library as both micro arrays on glass slides and in well-plates, PBAE and monomer *G* were mixed with diacrylates *A-F* (1:1 w/w ratio). The solvent (DMF, bp=153°C) and any eventual unreacted volatile monomer (i.e. *E*, bp=162°C) were removed after polymerization in a vacuum oven as indicated by surface chemical characterization techniques (ToF-SIMS, Supporting Information). The co-polymers are identified as diacrylate (*A-G*) with PBAE (from *A1* to *F6*), resulting in copolymers denoted in this form, *AA1* to *GF6*.

High throughput micro array assessment

The polymer microarrays were used to carry out high throughput cytotoxicity assessment, mechanical property measurements using atomic force microscopy (AFM) and surface chemical characterization (Figure 2) by ToF-SIMS (Supporting Information, Figures S15).^{30,29} High throughput measurement of the elastic modulus was achieved using automated AFM analysis of

the array (Figure 2b) by PeakForce quantitative nanomechanics (QNM) imaging mode, revealing a wide range of elastic moduli throughout had been achieved on the polymer library.



1
2
3 under investigation, no component showed a specifically detrimental effect so all material
4 chemistries went forward for further consideration.
5
6

7
8 Polymer mechanical properties are relevant to biomaterial application, and consequently we
9 have developed a high throughput method to determine stiffness modulus from the micro array
10 format and provide choice of material further downstream.³⁶⁻⁴⁰ AFM has previously been used in
11 a high-throughput to morphologically characterize polymer micro arrays but not previously to
12 determine modulus.³⁴ PeakForce QNM, which allows simultaneous imaging and mechanical
13 property measurement was used to automatically analyze all the spots on the microarray. The
14 information acquired provides the Derjaguin–Muller–Toporov (DMT) modulus^{41,42} amongst
15 other sample properties. Cantilevers suitable for the measurement of moduli between 5 and 2000
16 MPa were used to obtain quantitative measurements across most of the polymers (see Supporting
17 Information for details).⁴²⁻⁴⁵ Due to the uncertainty of the geometrical models used to represent
18 the probe tips, it is most appropriate to present these data as ranges of elastic moduli instead of
19 discrete values (Figure 2b). Moduli were measured ranging from 1 MPa to 5 GPa. To put these
20 moduli in context, medical polyurethanes fall in the range of 5-7 MPa, PDMS ranges from 48
21 kPa up to 2 MPa,⁴⁶ mixtures of PDMS and polyurethane are used measuring a few (15-35)
22 MPa,⁴⁷ subcutaneous tissue around 4 kPa,⁴⁸ dermis 2.8-4 MPa⁴⁹ and human bone is found in the
23 range of 3-20 GPa.⁵⁰ Flexible and intermediate modulus materials with a stiffness in the MPa
24 range are thought to be most suitable for subcutaneous implantation to achieve a balance of
25 mechanical stability and flexibility.⁴⁷ The range of material moduli achieved in this library of
26 bioresorbable materials offers a route to tuning the material to the desired function.
27
28
29
30
31
32
33
34
35
36
37
38
39
40
41
42
43
44
45
46
47
48
49
50
51
52
53

54 **Library fabrication in well plates for drug release quantification**

55
56
57
58
59
60

1
2
3 Ready determination of drug release requires separate compartments into which the eluted
4 drug can be collected and quantified in solution. Consequently, the library was photocured in a
5 384 well-plate format, where each well contained a solution of the drug and the photo initiator
6 [2% in DMF, 2,2-dimethoxy-2-phenylacetophenone (DMPA)] added to the diacrylate-PBAE
7 mixtures in 70% DMF (w/v), so as to achieve 100 ng of drug per well. The drug loading was
8 chosen such that the release concentration was within limits required in the body.^{51,52} After UV
9 curing and vacuum drying, the samples were incubated in 100 μ L phosphate buffered saline
10 (PBS, pH 7.4). At selection times, 75 μ L of the dissolution media was transferred to black
11 polystyrene plates for fluorescence measurements ($\lambda_{\text{ex}}=270$, $\lambda_{\text{em}}=335$) by using an automatic
12 pipetting robot (Biotek). The experiments were performed in triplicate and included a control
13 plate containing the (co)polymers without drug as a background. The release profiles for the
14 materials are presented in Figure 3a for times up to 2 months. These reveal a wide range of
15 release rates from the polymers: for ease of visual interpretation, only the 20 h and 2 month time
16 points of release are shown from the 1 h time point measurements made up to 2 months (Figures
17 S1-S6).
18
19
20
21
22
23
24
25
26
27
28
29
30
31
32
33
34
35
36
37
38
39
40
41
42
43
44
45
46
47
48
49
50
51
52
53
54
55
56
57
58
59
60

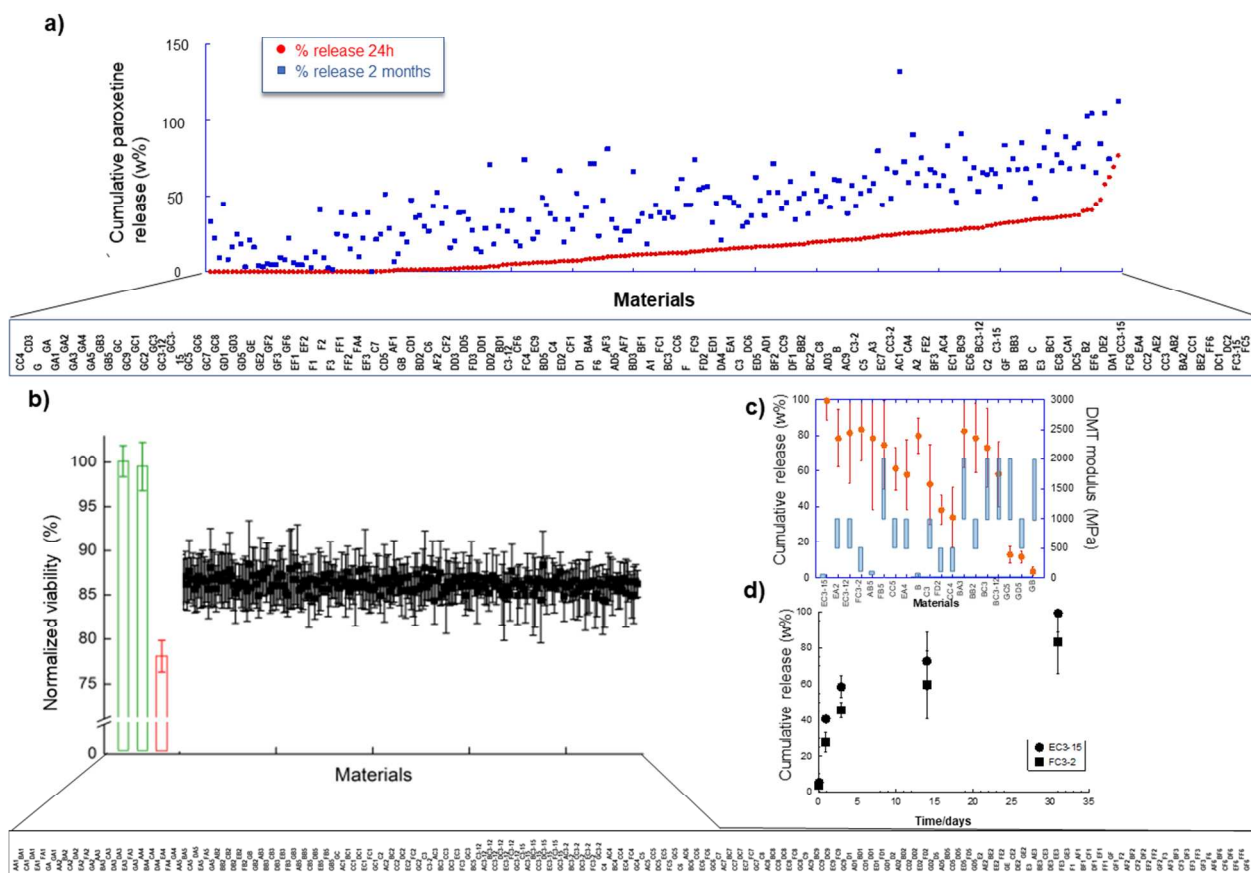


Figure 3. (a) Cumulative paroxetine release for the materials ordered from lower (left) to higher (right) cumulative release at 20h (red). Release after 2 months (64 days) is depicted in blue. (b) Normalized cell viability quantified from the Neutral Red stain for the PBAE materials. Green bars show negative controls (left to right: bare glass and pHEMA-coated glass), the red bar the positive control (cyanoacrylate adhesive). (c) Release profile after one month (31 days, orange dots) and AFM determined elastic modulus intervals (blue bars) for 19 materials. (d) Cumulative kinetic release profile for 2 of the hit materials, over 31 days. All error bars depict standard deviation from the mean.

1
2
3 A number of materials, desirable for extended release in that they follow a near zero-order^{53,54}
4 release profile were identified (Figure 3). Nineteen polymers were selected as of interest based
5 on linear release profile. All of them also showed an initial burst release (Figure 3 and Figure S7)
6 commonly observed in commercial formulations of drugs from polymer drug delivery
7 matrices^{53,11} including polyurethane (PU),⁵⁵ polydimethylsiloxane (PDMS)^{56,57} or poly(ethylene
8 vinyl acetate),⁵⁸ PLGA and methacrylate based materials.⁵³ This is beneficial in some situations,
9 in the case of paroxetine, an initial amount in blood might be desirable to reach a therapeutic
10 level rapidly.
11
12
13
14
15
16
17
18
19
20
21
22
23

24 **Printability screening**

25
26 In order to test printability in a piezo electric system, a number of aspects of the ink
27 formulations needed to be considered. Firstly, the 19 candidate materials showing near zero
28 order release were reduced to 9 combinations based on the solubility of the PBAE in the
29 diacrylate monomer without any additional solvent-for maximum simplicity, resulting in the use
30 of only PBAE materials based on C and A. The resulting 9 combinations were then screened
31 using the criteria of ejection from an automated piezo electric microarray printer (SciFlexarrayer
32 S5, Scenion). This has similarities with inkjet 3D printers, but with the advantage of being able
33 to simultaneously screen multiple inks utilising just 50 μ l of each from a well plate in a fully
34 automated manner. Although the high viscosity of our formulations does not allow for a high-
35 throughput printability screening by using system, it may be applied to low viscosity
36 formulations in high-throughput format. Solvent dilution was used as a surrogate for increased
37 temperature to reduce viscosity in the 3D printer. The inks were prepared at 6.25%, 12.5%, 25%
38 and 50% in DMF (w/v) and 50 μ l of each solution was transferred into 384 well plate (See
39
40
41
42
43
44
45
46
47
48
49
50
51
52
53
54
55
56
57
58
59
60

1
2
3 Supporting Information for details). Although all the inks could be aspirated and ejected under
4 almost all levels of dilution, the drug was readily soluble in only the most hydrophilic monomers
5
6 (*D-F*). From the 4 inks that dissolve the drug, only *FC3-2* and *EC3-15* could be ejected as drops
7
8 at the minimum dilution and thus at the lowest temperature (Table 1 and Figure S9).
9
10 Interestingly, these formulations involve both the *C3* PBAE (tripropylene glycol combined with
11
12 triethylamine at different ratios) copolymerized with polyethylene glycol (MW=500) and
13
14 diethylene glycol (*F* and *E*, Figure 1) respectively. Several PBAE prepared from tripropylene
15
16 glycol appear to be miscible with several diacrylates giving formulations suitable to be printed.
17
18 These were therefore assessed to be the formulations most likely ready to be printed by using the
19
20 original screened formulation without further adjustments for viscosity (i.e. increasing
21
22 diacrylate/PBAE ratio). The elastic modulus of these was also within the MPa range (Figure 3c),
23
24 suitable to prepare drug delivery subcutaneous implants.⁴⁷ This method was able to predict the
25
26 two formulations ultimately found to be printable, indicating its suitability for rapid assessment
27
28 of candidate materials for 3D printing.
29
30
31
32
33
34
35
36
37
38
39
40
41
42
43
44
45
46
47
48
49
50
51
52
53
54
55
56
57
58
59
60

Table 1. Printability screening results (A= aspirated and E= ejected) for the 9 inks prepared at 25% and 50% in DMF (w/v).

Ink (%) ^[a]	25%		50%	
Ink	A	E	A	E
<i>BA3</i>	x	x	x	x
<i>BC3</i>	√	√	x	x
<i>C3</i>	√	√	x	x
<i>CC4</i>	√	√	x	x
<i>CC5</i>	√	√	x	x
<i>EA2</i>	√	x	x	x
<i>FC3-2</i>	√	√	√	√
<i>EC3-12</i>	√	√	x	x
<i>EC3-15</i>	√	√	√	x

^[a] Percentage of the ink in the formulation with DMF

Scale up of hit polymers using UV photo initiated inkjet printing

As a consequence of the screening protocols, the two formulations identified (*FC3-2* and *EC3-15*) were shown to produce materials with a near-zero order release profile (Figure 3cd) and were suitable for 3D printing (Table 1). Additionally, they proved to be non-toxic to cells (Figure 2b and S8) and the modulus was within the range of commonly utilized biomedical elastomers (Figure 3c)^{47,11}. Both the measured viscosity and the surface tension of the ink formulations selected for scale up were in the appropriate range for printability, both with and without drug at a temperature of 60°C, i.e. between 10-13 cP, with the range of 9-15 cP recognized as optimal²² (Table 2 and Figure S12). The two candidate materials were found to be dispensable on a commercial inkjet printer (Dimatix DMP 2800) by using standard waveforms (suitable to print

commercial UV curable inks) where single spherical drops without satellites were achievable just through the adjustment of the cartridge working temperature (between 25 and 70°C in all cases). In order to test the predictability of our printability screening, an ink predicted to not be printable from the high throughput test (*BA3* in Table 1) was checked for dispensing, and was found not to be printable on the Dimatix DMP 2800 by using standard waveforms at the highest temperature available (70 °C), giving us confidence that our method is able to discriminate between inks that can and can't be used for 3D printing. Scale up was demonstrated by successfully printing different objects from both inks (Figure 4c-h) on polyethylene terephthalate (PET) foil using 6 of the available 16 nozzles simultaneously, with curing initiated through concurrent illumination of UV during each pass of the print head. Simple objects of various geometries were produced including squares, rectangles, grids and a honeycomb using the number of layers to control thickness between 0.1 to 0.6mm; control of architecture is a powerful route to control release.⁵⁹

Table 2. Viscosity at printing temperatures and surface tension measured both with and without drug incorporated paroxetine in the ink formulation.

	<i>FC3-2</i>	<i>EC3-15</i>
Viscosity [MPa.s] ^[a]	13.18±0.36	10.61±0.10
Surface tension [mN.m ⁻¹] ^[b]	32.81±0.21	31.96±0.11
Surface tension [mN.m ⁻¹] ^[c]	33.11±0.23	32.75±0.38

^[a]Data at printing temperature (60 C); ^[b] RT; ^[c] RT containing 1 mg/mL paroxetine hydrochloride.

A full object characterization involving drug release, polymer degradability and mechanical characterization for the *FC3-2* material was achieved by printing cm sized squares (25 layers,

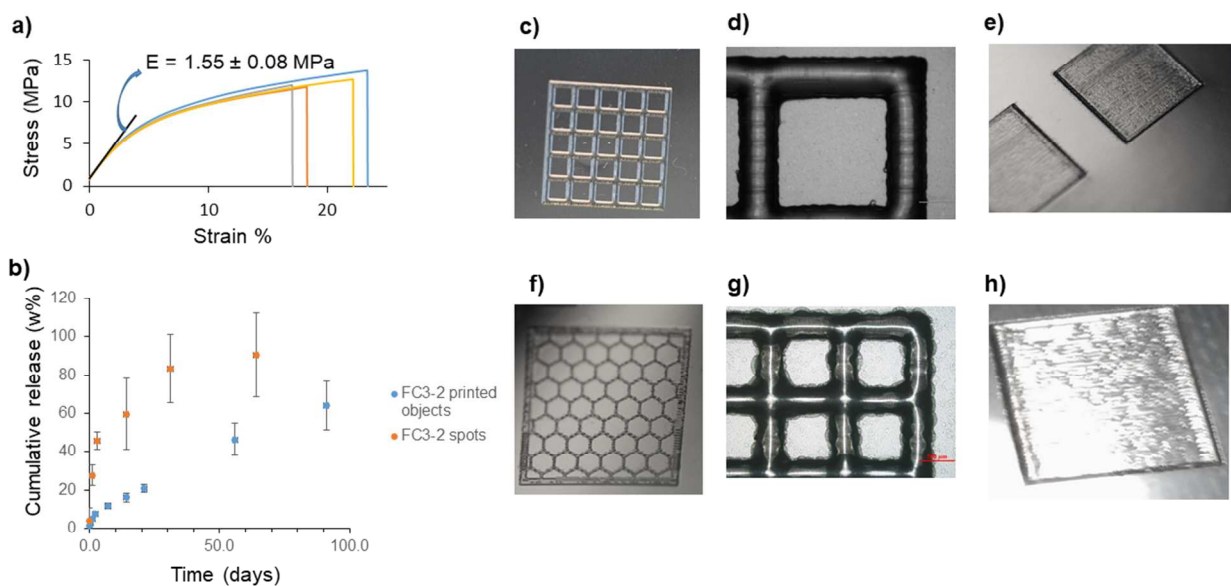
1
2
3 113 μm thick, 1x1 cm) and rectangles (30 layers, 137 μm thick, 1x2.5 cm) (Figures 4b, S10 and
4
5 4a respectively). The tensile test moduli measurements revealed an average elastic modulus of
6
7 1.55 \pm 0.08 MPa (Figure 4a, see Supporting Information for details), within the range of
8
9 biomedical used elastomers. This result is one order of magnitude lower than the surface DMT
10
11 modulus estimated by Peak Force QNM AFM. Such difference between nanoscale surface and
12
13 bulk measurements are not uncommon, reflecting both the very different methods used and that
14
15 the surface can have quite different physical properties to the bulk. This does not detract from the
16
17 utility of the AFM based approach to achieve high throughput screening of a large number of
18
19 materials using their relative moduli measurements.
20
21
22
23
24
25

26 Drug release and degradability experiments were performed with 5 replicates of 1 cm^2 printed
27
28 squares of FC3-2 (25 layers) by immersing the printed materials in PBS to such a volume that
29
30 upon elution of all drug the concentration reached would be 10 $\mu\text{g}/\text{mL}$, and incubated at 37°C
31
32 (Figure 4b). The thin film geometry was selected as a simple starting point from which shape can
33
34 be adjusted in the future for fine-tuning of drug release according to personalized requirements.
35
36 The linear behavior and burst effect is maintained when scaling-up, which illustrates the success
37
38 and suitability of the screening methodology proposed.
39
40
41

42 The current demonstration system is suitable for commencing *in vitro* studies to assess the
43
44 actual effect of geometry *in vivo* and in preclinical animal models.
45
46

47 For a future local implant, those devices show the potential to maintain a therapeutically local
48
49 drug concentration over at least three months. Hydrolytic degradation experiments with
50
51 analogous samples without incorporating the drug were performed (Figure S14). The mass loss
52
53 recorded on an initially weekly, then bi-weekly basis showed a degradation of the polymer
54
55
56
57
58
59
60

1
2
3 slower than the drug release. This is consistent with polymer degradation not being the only
4 mechanism of release, but rather diffusion of the active from the polymer plays a major role as
5 observed for commercially biodegradable polymers.⁶⁰
6
7
8
9
10
11
12
13
14
15



35
36 **Figure 4.** (a) Results of tensile experiments (4 replicates) representing stress (MPa) vs.
37 percentage of strain. The slope of the linear part is the elastic Young modulus (E). (b)
38 Comparison of the cumulative paroxetine release profile of *FC3-2* printed 1 cm² squares (25
39 layers, 5 replicates, blue) and HT screening in well plates (orange, 3 replicates. Note that the
40 release should be completed at day 42, prior to the last measurement). (c- h) Exemplary pictures
41 (c, e, f, h) and micrographs (d,g) of printed structures: (c) *FC3-2* grid, 99 and (d) 50 layers, (e)
42 *FC3-2* 1x1 cm 25-layer squares, (f) 1x1 cm 5-layer honeycomb (g) *EC3-15* grid, 20 layers and
43 *FC3-2* 1x1 cm 25-layer squares, (f) 1x1 cm 5-layer honeycomb (g) *EC3-15* grid, 20 layers and
44 *FC3-2* 1x1 cm 25-layer squares, (f) 1x1 cm 5-layer honeycomb (g) *EC3-15* grid, 20 layers and
45 *FC3-2* 1x1 cm 25-layer squares, (f) 1x1 cm 5-layer honeycomb (g) *EC3-15* grid, 20 layers and
46 *FC3-2* 1x1 cm 25-layer squares, (f) 1x1 cm 5-layer honeycomb (g) *EC3-15* grid, 20 layers and
47 *FC3-2* 1x1 cm 25-layer squares, (f) 1x1 cm 5-layer honeycomb (g) *EC3-15* grid, 20 layers and
48 *FC3-2* 1x1 cm 25-layer squares, (f) 1x1 cm 5-layer honeycomb (g) *EC3-15* grid, 20 layers and
49 *FC3-2* 1x1 cm 25-layer squares, (f) 1x1 cm 5-layer honeycomb (g) *EC3-15* grid, 20 layers and
50 *FC3-2* 1x1 cm 25-layer squares, (f) 1x1 cm 5-layer honeycomb (g) *EC3-15* grid, 20 layers and
51 *FC3-2* 1x1 cm 25-layer squares, (f) 1x1 cm 5-layer honeycomb (g) *EC3-15* grid, 20 layers and
52 *FC3-2* 1x1 cm 25-layer squares, (f) 1x1 cm 5-layer honeycomb (g) *EC3-15* grid, 20 layers and
53 *FC3-2* 1x1 cm 25-layer squares, (f) 1x1 cm 5-layer honeycomb (g) *EC3-15* grid, 20 layers and
54 *FC3-2* 1x1 cm 25-layer squares, (f) 1x1 cm 5-layer honeycomb (g) *EC3-15* grid, 20 layers and
55 *FC3-2* 1x1 cm 25-layer squares, (f) 1x1 cm 5-layer honeycomb (g) *EC3-15* grid, 20 layers and
56 *FC3-2* 1x1 cm 25-layer squares, (f) 1x1 cm 5-layer honeycomb (g) *EC3-15* grid, 20 layers and
57 *FC3-2* 1x1 cm 25-layer squares, (f) 1x1 cm 5-layer honeycomb (g) *EC3-15* grid, 20 layers and
58 *FC3-2* 1x1 cm 25-layer squares, (f) 1x1 cm 5-layer honeycomb (g) *EC3-15* grid, 20 layers and
59 *FC3-2* 1x1 cm 25-layer squares, (f) 1x1 cm 5-layer honeycomb (g) *EC3-15* grid, 20 layers and
60 *FC3-2* 1x1 cm 25-layer squares, (f) 1x1 cm 5-layer honeycomb (g) *EC3-15* grid, 20 layers and

Conclusions

In summary, we have developed the first high-throughput screening methodology to identify 3D printable inks, exemplified here using UV curable bioresorbable co-polymers with drug release properties relevant to releasing implants; near zero order release profile compatible with drug concentration close to therapeutic levels. The 3D printability of hit materials was assessed to identify inks for scale up to objects that exhibited extended and linear drug release profiles achieving therapeutic concentrations and appropriate elastic modulus for biomedical devices. The UV initiated inkjet printing approach was used to achieve different object geometries illustrating the flexibility of form that can be achieved. High throughput cytotoxicity experiments were developed based on polymer micro arrays on which high throughput elastic modulus measurements were also undertaken for the first time. This information was complemented by applying ToF SIMS as high throughput surface chemical characterisation method. The methodology described herein is proposed as a robust tool to identify novel printable functional materials which we see being of great utility to the emergence of 3D printing in biomedicine and may readily be combined with other high-throughput material screening methods in the biomaterials field such as cell attachment, bacterial resistance and immune modulation.

ASSOCIATED CONTENT

Supporting Information. Experimental details regarding poly- β -amino ester (PBAE) synthesis, microarray preparation, screening for drug release kinetics, atomic force microscopy, screening for PBAE-array cytotoxicity, screening for printability, 3D printing, rheology and surface tension measurements, drug release of printed materials, degradability experiments by

1
2
3 dissolution, Time of Flight-Secondary Ion Mass Spectrometry (ToF-SIMS), Gel Permeation
4 Chromatography (GPC) and Nuclear Magnetic Resonance (NMR) spectra are supplied as
5
6 Supporting Information (PDF). The following files are available free of charge.
7
8
9

10 AUTHOR INFORMATION

11 12 13 14 **Corresponding Author**

15 *E-mail: morgan.alexander@nottingham.ac.uk
16
17
18
19

20 **Present Addresses**

21
22 † Centro Singular de Investigación en Química Biolóxica e Materiais Moleculares (CIQUS) and
23 Departamento de Química Orgánica, Universidade de Santiago de Compostela, Jenaro de la
24 Fuente s/n, Santiago de Compostela, 15782 (Spain)
25
26
27
28
29

30 **Author Contributions**

31
32 The manuscript was written through contributions of all authors. Iria Louzao carried out the bulk
33 of the experimental work and manuscript preparation for this paper with additional experiments
34 carried out by Britta Koch, Vincenzo Taresco, Laura Ruiz-Cantu. The work was conceived,
35 organised and made possible with funding won by Clive J. Roberts, Christopher Tuck, Ricky
36 Wildman, Cameron Alexander, Richard Hague and Morgan R. Alexander. Manuscript drafting
37 and submission was led by Richard Hague, Cameron Alexander, Ricky Wildman and Morgan R.
38 Alexander. All authors have given approval to the final version of the manuscript.
39
40
41
42
43
44
45
46
47
48
49

50 **Funding Sources**

51
52 This work was funded by the EPSRC grants Multifunctional Additive Manufacturing
53 (EP/K005138/1), EPSRC Centre for Innovative Manufacturing in Additive Manufacturing
54
55
56
57
58
59
60

(EP/I033335/2), Programme Grant for Next Generation Biomaterials Discovery (EP/N006615/1) and Formulation for 3D printing: Creating a plug and play platform for a disruptive UK industry (EP/N024818/1).

Notes

The authors declare no competing financial interests.

ACKNOWLEDGMENT

Daniel G. Anderson (Massachusetts Institute of Technology) is acknowledged for his suggestion of using PBAEs as a bioresorbable polymeric library. The authors thank Dr. Xinyong Chen, Dr. Gemma Bray, Dr. David Scurr, Dr. Andrew Hook, Dr. Belen Begines, Annesi Giacaman and Dr. Ehab Saleh (University of Nottingham) for providing Excel macros to analyse AFM data, the gift of JCRB1149 human mesenchymal stem cells, their kind assistance with ToF-SIMS and Biodot dispensing system, providing waveforms for 3D printing, acquiring tensile strength data and kind assistance for acquiring some pictures of printed objects respectively.

ABBREVIATIONS

AFM atomic force microscopy, DMF dimethylformamide, DMPA 2,2-dimethyl-2-phenylacetophenone, DMT Derjaguin–Muller–Toporov, PBAE poly- β -amino esters, PBS phosphate buffered saline, PHEMA poly-hydroxyethylmethacrylate, PLGA poly-lactic-co-glycolic acid, QNM quantitative nanomechanics, ToF-SIMS Time-of-flight secondary ions mass spectrometry.

REFERENCES

- (1) He, Y.; Tuck, C. J.; Prina, E.; Kilsby, S.; Christie, S. D. R.; Edmondson, S.; Hague, R. J. M.; Rose, F. R. A. J.; Wildman, R. D. A New Photocrosslinkable Polycaprolactone-Based

- 1
2
3 Ink for Three-Dimensional Inkjet Printing. *J. Biomed. Mater. Res. - Part B Appl.*
4
5 *Biomater.* **2017**, *105* (6), 1645–1657.
6
7
8
9 (2) Hart, L. R.; Li, S.; Sturgess, C.; Wildman, R.; Jones, J. R.; Hayes, W. 3D Printing of
10
11 Biocompatible Supramolecular Polymers and Their Composites. *ACS Appl. Mater.*
12
13 *Interfaces* **2016**, *8* (5), 3115–3122.
14
15
16 (3) Chia, H. N.; Wu, B. M. Recent Advances in 3D Printing of Biomaterials. *J. Biol. Eng.*
17
18 **2015**, *9* (1), 4.
19
20
21 (4) He, Y.; Wildman, R. D.; Tuck, C. J.; Christie, S. D. R.; Edmondson, S. An Investigation
22
23 of the Behavior of Solvent Based Polycaprolactone Ink for Material Jetting. *Sci. Rep.*
24
25 **2016**, *6*, 20852.
26
27
28
29 (5) Guvendiren, M.; Molde, J.; Soares, R. M. D.; Kohn, J. Designing Biomaterials for 3D
30
31 Printing. *ACS Biomater. Sci. Eng.* **2016**, *2* (10), 1679–1693.
32
33
34
35 (6) Jose, R. R.; Rodriguez, M. J.; Dixon, T. A.; Omenetto, F.; Kaplan, D. L. Evolution of
36
37 Bioinks and Additive Manufacturing Technologies for 3D Bioprinting. *ACS Biomater.*
38
39 *Sci. Eng.* **2016**, *2* (10), 1662–1678.
40
41
42
43 (7) Nadgorny, M.; Xiao, Z.; Connal, L. A. 2D and 3D-Printing of Self-Healing Gels: Design
44
45 and Extrusion of Self-Rolling Objects. *Mol. Syst. Des. Eng.* **2017**, *2* (3), 283–292.
46
47
48
49 (8) Nadgorny, M.; Xiao, Z.; Chen, C.; Connal, L. A. Three-Dimensional Printing of pH-
50
51 Responsive and Functional Polymers on an Affordable Desktop Printer. *ACS Appl. Mater.*
52
53 *Interfaces* **2016**, *8* (42), 28946–28954.
54
55
56 (9) Bakarich, S. E.; Gorkin, R.; Panhuis, M. in het; Spinks, G. M. 4D Printing with
57
58
59
60

- 1
2
3 Mechanically Robust, Thermally Actuating Hydrogels. *Macromol. Rapid Commun.* **2015**,
4
5 36 (12), 1211–1217.
6
7
8
9 (10) Peterson, G. I.; Larsen, M. B.; Ganter, M. A.; Storti, D. W.; Boydston, A. J. 3D-Printed
10
11 Mechanochromic Materials. *ACS Appl. Mater. Interfaces* **2015**, 7 (1), 577–583.
12
13
14 (11) Anselmo, A. C.; Mitragotri, S. An Overview of Clinical and Commercial Impact of Drug
15
16 Delivery Systems. *J. Control. Release* **2014**, 190, 15–28.
17
18
19 (12) Kempin, W.; Franz, C.; Koster, L.-C.; Schneider, F.; Bogdahn, M.; Weitschies, W.;
20
21 Seidlitz, A. Assessment of Different Polymers and Drug Loads for Fused Deposition
22
23 Modeling of Drug Loaded Implants. *Eur. J. Pharm. Biopharm.* **2017**, 115 (Supplement C),
24
25 84–93.
26
27
28
29 (13) Khaled, S. A.; Burley, J. C.; Alexander, M. R.; Yang, J.; Roberts, C. J. 3D Printing of
30
31 Five-in-One Dose Combination Polypill with Defined Immediate and Sustained Release
32
33 Profiles. *J. Control. Release* **2015**, 217, 308–314.
34
35
36
37 (14) Hutmacher, D. W. Scaffolds in Tissue Engineering Bone and Cartilage. *Biomaterials*
38
39 **2000**, 21 (24), 2529–2543.
40
41
42
43 (15) Gross, B. C.; Erkal, J. L.; Lockwood, S. Y.; Chen, C.; Spence, D. M. Evaluation of 3D
44
45 Printing and Its Potential Impact on Biotechnology and the Chemical Sciences. *Anal.*
46
47 *Chem.* **2014**, 86 (7), 3240–3253.
48
49
50
51 (16) ASTM International. *Standard Terminology for Additive Manufacturing -General*
52
53 *Principles-Terminology*; 2015.
54
55
56 (17) Spears, B. R.; Marin, M. A.; Chaker, A. N.; Lampley, M. W.; Harth, E. Precise
57
58
59
60

- 1
2
3 Microscale Polymeric Networks through Piezoelectronic Inkjet Printing. *ACS Biomater.*
4
5 *Sci. Eng.* **2016**, *2* (8), 1265–1272.
6
7
8
9 (18) Tao, H.; Marelli, B.; Yang, M.; An, B.; Onses, M. S.; Rogers, J. A.; Kaplan, D. L.;
10 Omenetto, F. G. Inkjet Printing of Regenerated Silk Fibroin: From Printable Forms to
11 Printable Functions. *Adv. Mater.* **2015**, *27* (29), 4273–4279.
12
13
14
15
16 (19) Kolesky, D. B.; Truby, R. L.; Gladman, A. S.; Busbee, T. A.; Homan, K. A.; Lewis, J. A.
17 3D Bioprinting of Vascularized, Heterogeneous Cell-Laden Tissue Constructs. *Adv.*
18 *Mater.* **2014**, *26* (19), 3124–3130.
19
20
21
22
23
24 (20) Sydney Gladman, A.; Matsumoto, E. A.; Nuzzo, R. G.; Mahadevan, L.; Lewis, J. A.
25 Biomimetic 4D Printing. *Nat Mater* **2016**, *15* (4), 413–418.
26
27
28
29 (21) Kolesky, D. B.; Homan, K. A.; Skylar-Scott, M. A.; Lewis, J. A. Three-Dimensional
30 Bioprinting of Thick Vascularized Tissues. *Proc. Natl. Acad. Sci.* **2016**, *113* (12), 3179–
31 3184.
32
33
34
35
36
37 (22) Derby, B. Inkjet Printing of Functional and Structural Materials: Fluid Property
38 Requirements, Feature Stability, and Resolution. *Annu. Rev. Mater. Res.* **2010**, *40* (1),
39 395–414.
40
41
42
43
44
45 (23) de Gans, B.-J.; Duineveld, P. C.; Schubert, U. S. Inkjet Printing of Polymers: State of the
46 Art and Future Developments. *Adv. Mater.* **2004**, *16* (3), 203–213.
47
48
49
50 (24) Anderson, D. G.; Tweedie, C. A.; Hossain, N.; Navarro, S. M.; Brey, D. M.; Van Vliet, K.
51 J.; Langer, R.; Burdick, J. A. A Combinatorial Library of Photocrosslinkable and
52 Degradable Materials. *Adv. Mater.* **2006**, *18* (19), 2614–2618.
53
54
55
56
57
58
59
60

- 1
2
3 (25) Green, J. J.; Zugates, G. T.; Tedford, N. C.; Huang, Y.-H.; Griffith, L. G.; Lauffenburger,
4 D. A.; Sawicki, J. A.; Langer, R.; Anderson, D. G. Combinatorial Modification of
5 Degradable Polymers Enables Transfection of Human Cells Comparable to Adenovirus.
6 *Adv. Mater.* **2007**, *19* (19), 2836–2842.
7
8
9
10
11
12
13 (26) Green, J. J.; Chiu, E.; Leshchiner, E. S.; Shi, J.; Langer, R.; Anderson, and D. G.
14 Electrostatic Ligand Coatings of Nanoparticles Enable Ligand-Specific Gene Delivery to
15 Human Primary Cells. *Nano Lett.* **2007**, *7* (4), 874–879.
16
17
18
19
20
21 (27) Group, D. U. A. Paroxetine: A Selective Serotonin Reuptake Inhibitor Showing Better
22 Tolerance, but Weaker Antidepressant Effect than Clomipramine in a Controlled
23 Multicenter Study. *J. Affect. Disord.* **1990**, *18* (4), 289–299.
24
25
26
27
28
29 (28) Grimsley, S. R.; Jann, M. W. Paroxetine, Sertraline, and Fluvoxamine: New Selective
30 Serotonin Reuptake Inhibitors. *Clin. Pharm.* **1992**, *11* (11), 930–957.
31
32
33
34 (29) Urquhart, A. J.; Anderson, D. G.; Taylor, M.; Alexander, M. R.; Langer, R.; Davies, M. C.
35 High Throughput Surface Characterisation of a Combinatorial Material Library. *Adv.*
36
37
38
39
40
41
42 (30) Algahtani, M. S.; Scurr, D. J.; Hook, A. L.; Anderson, D. G.; Langer, R. S.; Burley, J. C.;
43 Alexander, M. R.; Davies, M. C. High Throughput Screening for Biomaterials Discovery.
44
45
46
47
48
49
50 (31) Celiz, A. D.; Smith, J. G. W.; Langer, R.; Anderson, D. G.; Winkler, D. A.; Barrett, D. A.;
51 Davies, M. C.; Young, L. E.; Denning, C.; Alexander, M. R. Materials for Stem Cell
52
53
54
55
56
57
58
59
60

- 1
2
3 (32) Celiz, A. D.; Smith, J. G. W.; Patel, A. K.; Hook, A. L.; Rajamohan, D.; George, V. T.;
4 Flatt, L.; Patel, M. J.; Epa, V. C.; Singh, T.; Langer, R.; Anderson, D. G.; Allen, N. D.;
5 Hay, D. C.; Winkler, D. A.; Barrett, D. A.; Davies, M. C.; Young, L. E.; Denning, C.;
6 Alexander, M. R. Discovery of a Novel Polymer for Human Pluripotent Stem Cell
7 Expansion and Multilineage Differentiation. *Adv. Mater.* **2015**, *27* (27), 4006–4012.
8
9
10
11
12
13
14
15 (33) Hammad, M.; Rao, W.; Smith, J. G. W.; Anderson, D. G.; Langer, R.; Young, L. E.;
16 Barrett, D. A.; Davies, M. C.; Denning, C.; Alexander, M. R. Identification of Polymer
17 Surface Adsorbed Proteins Implicated in Pluripotent Human Embryonic Stem Cell
18 Expansion. *Biomater. Sci.* **2016**, *4* (9), 1381–1391.
19
20
21
22
23
24
25 (34) Hook, A. L.; Yang, J.; Chen, X.; Roberts, C. J.; Mei, Y.; Anderson, D. G.; Langer, R.;
26 Alexander, M. R.; Davies, M. C. Polymers with Hydro-Responsive Topography Identified
27 Using High Throughput AFM of an Acrylate Microarray. *Soft Matter* **2011**, *7* (16), 7194–
28 7197.
29
30
31
32
33
34
35 (35) Hawkins, A. M.; Milbrandt, T. A.; Puleo, D. A.; Hilt, J. Z. Synthesis and Analysis of
36 Degradation, Mechanical and Toxicity Properties of Poly(β -Amino Ester) Degradable
37 Hydrogels. *Acta Biomater.* **2011**, *7* (5), 1956–1964.
38
39
40
41
42
43 (36) Dean, M. N.; Swanson, B. O.; Summers, A. P. Biomaterials: Properties, Variation and
44 Evolution. *Integr. Comp. Biol.* **2009**, *49* (1), 15–20.
45
46
47
48 (37) Reilly, G. C.; Engler, A. J. Intrinsic Extracellular Matrix Properties Regulate Stem Cell
49 Differentiation. *J. Biomech.* **2010**, *43* (1), 55–62.
50
51
52
53
54 (38) Nair, L. S.; Laurencin, C. T. Biodegradable Polymers as Biomaterials. *Prog. Polym. Sci.*
55
56
57
58
59
60

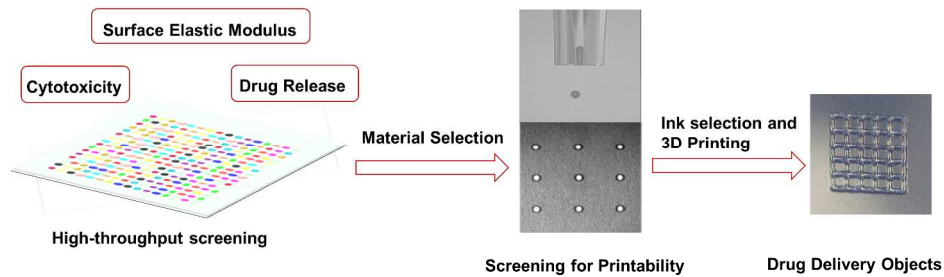
- 1
2
3 **2007**, 32 (8–9), 762–798.
- 4
5
6 (39) Mohanty, A. K.; Misra, M.; Hinrichsen, G. Biofibres, Biodegradable Polymers and
7 Biocomposites: An Overview. *Macromol. Mater. Eng.* **2000**, 276–277 (1), 1–24.
- 8
9
10
11 (40) Jain, R. A. The Manufacturing Techniques of Various Drug Loaded Biodegradable
12 Poly(lactide-Co-Glycolide) (PLGA) Devices. *Biomaterials* **2000**, 21 (23), 2475–2490.
- 13
14
15
16 (41) Derjaguin, B. V; Muller, V. M.; Toporov, Y. U. P. Effect of Contact Deformations on the
17 Adhesion of Particles. *J Colloid Interface Sci* **1975**, 53 (2), 314–326.
- 18
19
20
21
22 (42) Dokukin, M. E.; Sokolov, I. Quantitative Mapping of the Elastic Modulus of Soft
23 Materials with HarmoniX and Peak Force QNM AFM Modes. *Langmuir* **2012**, 28 (46),
24 16060–16071.
- 25
26
27
28
29 (43) Dokukin, M. E.; Sokolov, I. On the Measurements of Rigidity Modulus of Soft Materials
30 in Nanoindentation Experiments at Small Depth. *Macromolecules* **2012**, 45 (10), 4277–
31 4288.
- 32
33
34
35
36 (44) Clifford, C. A.; Seah, M. P. Quantification Issues in the Identification of Nanoscale
37 Regions of Homopolymers Using Modulus Measurement via AFM Nanoindentation.
38 *Appl. Surf. Sci.* **2005**, 252 (5), 1915–1933.
- 39
40
41
42
43 (45) Jee, A.-Y.; Lee, M. Comparative Analysis on the Nanoindentation of Polymers Using
44 Atomic Force Microscopy. *Polym. Test.* **2010**, 29 (1), 95–99.
- 45
46
47
48
49 (46) Brown, X. Q.; Ookawa, K.; Wong, J. Y. Evaluation of Polydimethylsiloxane Scaffolds
50 with Physiologically-Relevant Elastic Moduli: Interplay of Substrate Mechanics and
51 Surface Chemistry Effects on Vascular Smooth Muscle Cell Response. *Biomaterials* **2005**,
52
53
54
55
56
57
58
59
60

- 1
2
3 26 (16), 3123–3129.
4
5
6 (47) Simmons, A.; Padsalgikar, A. D.; Ferris, L. M.; Poole-Warren, L. A. Biostability and
7
8 Biological Performance of a PDMS-Based Polyurethane for Controlled Drug Release.
9
10 *Biomaterials* **2008**, *29* (20), 2987–2995.
11
12
13 (48) Iatridis, J. C.; Wu, J.; Yandow, J. A.; Langevin, H. M. Subcutaneous Tissue Mechanical
14
15 Behavior Is Linear and Viscoelastic under Uniaxial Tension. *Connect. Tissue Res.* **2003**,
16
17 *44* (5), 208–217.
18
19
20 (49) Zahouani, H.; Pailler-Mattei, C.; Sohm, B.; Vargiolu, R.; Cenizo, V.; Debret, R.
21
22 Characterization of the Mechanical Properties of a Dermal Equivalent Compared with
23
24 Human Skin in Vivo by Indentation and Static Friction Tests. *Ski. Res. Technol.* **2009**, *15*
25
26 (1), 68–76.
27
28
29 (50) Staiger, M. P.; Pietak, A. M.; Huadmai, J.; Dias, G. Magnesium and Its Alloys as
30
31 Orthopedic Biomaterials: A Review. *Biomaterials* **2006**, *27* (9), 1728–1734.
32
33
34 (51) Bourin, M.; Chue, P.; Guillon, Y. Paroxetine: A Review. *CNS Drug Rev.* **2001**, *7* (1), 25–
35
36 47.
37
38
39 (52) Tasker, T. C. G.; Bye, C. M.; Zussman, B. D.; Link, C. G. G. Paroxetine Plasma Levels:
40
41 Lack of Correlation with Efficacy or Adverse Events. *Acta Psychiatr. Scand.* **1989**, *80*
42
43 (S350), 152–155.
44
45
46 (53) Huang, X.; Brazel, C. S. On the Importance and Mechanisms of Burst Release in Matrix-
47
48 Controlled Drug Delivery Systems. *J. Control. Release* **2001**, *73* (2–3), 121–136.
49
50
51 (54) Fu, Y.; Kao, W. J. Drug Release Kinetics and Transport Mechanisms of Non-Degradable
52
53
54
55
56
57
58
59
60

- 1
2
3 and Degradable Polymeric Delivery Systems. *Expert Opin. Drug Deliv.* **2010**, 7 (4), 429–
4
5 444.
6
7
8
9 (55) Kang, E.; Vedantham, K.; Long, X.; Dadara, M.; Kwon, I.-K.; Sturek, M.; Park, K. Drug-
10 Eluting Stent for Delivery of Signal Pathway-Specific 1,3-Dipropyl-8-Cyclopentyl
11 Xanthine. *Mol. Pharm.* **2009**, 6 (4), 1110–1117.
12
13
14
15
16 (56) Woolfson, A. D.; Malcolm, R. K.; Morrow, R. J.; Toner, C. F.; McCullagh, S. D.
17 Intravaginal Ring Delivery of the Reverse Transcriptase Inhibitor {TMC} 120 as an
18 {HIV} Microbicide. *Int. J. Pharm.* **2006**, 325 (1–2), 82–89.
19
20
21
22
23
24 (57) Malcolm, R. K.; Woolfson, A. D.; Toner, C. F.; Morrow, R. J.; McCullagh, S. D. Long-
25 Term, Controlled Release of the HIV Microbicide TMC120 from Silicone Elastomer
26 Vaginal Rings. *J. Antimicrob. Chemother.* **2005**, 56 (5), 954–956.
27
28
29
30
31
32 (58) Arnold, R. R.; Wei, H. H.; Simmons, E.; Tallury, P.; Barrow, D. A.; Kalachandra, S.
33 Antimicrobial Activity and Local Release Characteristics of Chlorhexidine Diacetate
34 Loaded within the Dental Copolymer Matrix, Ethylene Vinyl Acetate. *J. Biomed. Mater.*
35 *Res. Part B Appl. Biomater.* **2008**, 86B (2), 506–513.
36
37
38
39
40
41
42 (59) Kyobula, M.; Adedeji, A.; Alexander, M. R.; Saleh, E.; Wildman, R.; Ashcroft, I.; Gellert,
43 P. R.; Roberts, C. J. 3D Inkjet Printing of Tablets Exploiting Bespoke Complex
44 Geometries for Controlled and Tuneable Drug Release. *J. Control. Release* **2017**, 261,
45 207–215.
46
47
48
49
50
51
52 (60) Lao, L. L.; Venkatraman, S. S.; Peppas, N. A. Modeling of Drug Release from
53 Biodegradable Polymer Blends. *Eur. J. Pharm. Biopharm.* **2008**, 70 (3), 796–803.
54
55
56
57
58
59
60

1
2
3
4
5
6
7
8
9
10
11
12
13
14
15
16
17
18
19
20
21
22
23
24
25
26
27
28
29
30
31
32
33
34
35
36
37
38
39
40
41
42
43
44
45
46
47
48
49
50
51
52
53
54
55
56
57
58
59
60

1
2
3
4
5
6
7
8
9
10
11
12
13
14
15
16
17
18
19
20
21
22
23
24
25
26
27
28
29
30
31
32
33
34
35
36
37
38
39
40
41
42
43
44
45
46
47
48
49
50
51
52
53
54
55
56
57
58
59
60



TOC

840x360mm (96 x 96 DPI)